


Ce₂Ir₃Ga₅ : A new locally noncentrosymmetric heavy fermion systemArushi ^{*}, Raul Cardoso-Gil, and Christoph Geibel*Max-Planck Institute for Chemical Physics of Solids, 01187 Dresden, Germany*

(Received 27 November 2023; accepted 25 July 2024; published 16 August 2024)

Recently, a new type of unconventional superconductivity with a field-induced transition between two different superconducting (SC) states was discovered in the heavy fermion system CeRh₂As₂. This unusual SC state was proposed to be based on specific symmetries of the underlying structure, i.e., a globally centrosymmetric layered structure, but where the Ce layers themselves lack inversion symmetry. This new type of SC state has attracted strong interest, prompting the search for further heavy fermion systems crystallizing in structures with appropriate symmetries. We report the discovery and the study of a new Ce-based heavy fermion system with a globally centrosymmetric structure but without inversion symmetry on the Ce-site, Ce₂Ir₃Ga₅. A single crystal x-ray diffraction study revealed an orthorhombic U₂Co₃Si₅ type structure. Resistivity, specific heat, and magnetization measurements indicate a moderate-heavy fermion behavior with a Kondo energy scale of the order of 40 K. Most experimental results suggest the absence of magnetic order, but a tiny anomaly in the specific heat opens the possibility for a very weak, itinerant type of ordering.

DOI: [10.1103/PhysRevMaterials.8.085001](https://doi.org/10.1103/PhysRevMaterials.8.085001)**I. INTRODUCTION**

In the past 20 years, the absence of inversion symmetry (IS) has emerged as an effective parameter to induce unusual superconducting properties and unconventional superconducting states [1,2]. Expected and reported effects are particularly strong in so-called heavy fermion systems [3,4]. Here, the strong electronic correlation effects emerging from the hybridization between localized *f* electrons, e.g., from Ce, Yb, or U-atoms, and itinerant valence electrons results in the formation of quasiparticles with huge effective masses at the Fermi level, with profound consequences on electric transport and thermodynamic properties. Among others, the enormous effective masses result in large SC critical fields (H_{c2}) of several Teslas despite very low SC transition temperatures (T_c) in the order of 0.5 K [5,6]. The absence of IS can then induce further unusually strong effects on these SC properties. Evidence of a strong influence of the absence of IS was first reported for a series of compounds crystallizing in BaNiSn₃ structure such as CeIrSi₃, CeRhSi₃, CeCoGe₃, and CeIrGe₃, where superconductivity under pressure was observed to present huge H'_{c2} s with a large anisotropy [6–9]. These unusual SC properties are assumed to emerge from the absence of IS in the structure of these compounds. Furthermore, the lack of an inversion symmetry also gives rise to

unconventional magnetic [10–13] and normal state properties [14].

Later on, theoretical studies indicated that even in globally centrosymmetric structures, the absence of an inversion symmetry on a local level can induce unusual SC states [15–18]. Thus, in layered structures without inversion symmetry in the layers but inversion symmetry for the whole structure, the latter results in an additional quantum number: the parity of the electronic states respective to the inversion center. Theoretical studies demonstrated the possibility of forming an unconventional SC state with odd parity in zero fields, which gets replaced by an even-parity SC state under an appropriate magnetic field [19–21]. The latter one presents a huge H_{c2} anisotropy. Remarkably, exactly such an unconventional SC phase diagram was recently observed in the heavy fermion system CeRh₂As₂ [22]. The nature of the unusual SC and normal state properties of CeRh₂As₂ are now the subject of strong interest and intense research [23–27].

An obvious question is whether similar unconventional and intriguing properties can be found in other heavy fermion systems with a global inversion symmetric structure but without IS on the Ce site. There are several Ce compounds with appropriate structures, but only some are appropriate for the search for unconventional superconductivity. For a Ce compound to be a promising candidate, its strength of the interaction between the 4*f* and conduction electrons, i.e., the *f-c* hybridization, has to be fine-tuned to put the system close to the so-called quantum critical point (QCP), where the *f-c* hybridization is just sufficiently strong to destroy the magnetic order, resulting in a transition to a paramagnetic ground state. Heavy fermion behavior and unconventional superconductivity are only expected and observed in the vicinity of such a QCP. Ce, Yb, or U compounds with suitable structural properties and appropriate strength of the *f-c* hybridization are very scarce [18,22,28,29].

*Contact author: arushi@cpfs.mpg.de

Published by the American Physical Society under the terms of the [Creative Commons Attribution 4.0 International license](https://creativecommons.org/licenses/by/4.0/). Further distribution of this work must maintain attribution to the author(s) and the published article's title, journal citation, and DOI. Open access publication funded by Max Planck Society.

In a search for appropriate systems, we explored the ternary Ce-Ir-Ga phase diagram. Combining the Ir and Ga ligands seemed to be a promising approach since Ir promotes a quite strong f - c hybridization, while Ga induces a comparatively weak one. This search leads to the discovery of a yet-unknown compound, $\text{Ce}_2\text{Ir}_3\text{Ga}_5$. X-ray diffraction demonstrated that it crystallizes in the $\text{U}_2\text{Co}_3\text{Si}_5$ structure type, which is globally centrosymmetric, but where the (crystallographic unique) Ce site lacks inversion symmetry. Electrical resistivity, magnetic susceptibility, and specific heat measurements evidenced a sizable f - c hybridization, resulting in a corresponding Kondo energy scale of the order of 40 K. Further properties suggest that $\text{Ce}_2\text{Ir}_3\text{Ga}_5$ is on the paramagnetic side of the QCP and presents a heavy Fermi liquid ground state. However, a weak anomaly in the specific heat could be an indication of a very weak magnetic order of itinerant $4f$ electrons. We could not yet observe superconductivity, which may be due to a too-large residual resistivity. In many cases, unconventional superconductivity in strongly correlated electron systems was observed to be very sensitive to the residual resistivity ratio (RRR), requiring a RRR larger than 50. The RRR in our present sample is about 5, thus one order of magnitude smaller.

II. EXPERIMENTAL DETAILS

For the synthesis of the $\text{Ce}_2\text{Ir}_3\text{Ga}_5$ samples, we started with the constituent elements Ce (99.99%), Ir (99.99%), and Ga (99.999%). Ce and Ir were taken in the stoichiometric ratio, while for Ga, we added 1% extra to compensate for evaporation losses. A differential thermal analysis (DTA) study indicated a congruent melting at 1340 °C. Accordingly, we tried two different methods for the preparation of this compound. The first method involves melting the elements in an arc furnace under an argon atmosphere. The resulting ingot was flipped over and remelted, and the same procedure was repeated four to five times to ensure homogeneity. In the second method, we used the prereacted ingot obtained by arc melting, crushed it into small pieces, and transferred it into a carbon crucible enclosed in a tantalum cylinder. The tantalum cylinder was then closed using an arc furnace under an argon atmosphere of 800 mbar. The whole crucible was then put in a resistance furnace, and the following heat treatment was applied: ramped up to 1380 °C, dwelled for 15 minutes, and then slowly cooled to room temperature. Both methods lead to a phase pure $\text{Ce}_2\text{Ir}_3\text{Ga}_5$ sample. Since, to the best of our knowledge, this compound has not been reported before, its crystallographic structure was determined using both single-crystal and powder x-ray diffraction (XRD). Single-crystal XRD data was obtained from a Rigaku AFC7 diffractometer system (MoK_α radiation, $\lambda = 0.71073 \text{ \AA}$), whereas powder XRD pattern was collected using a Stoe-Stadi-MP powder diffractometer in transmission mode equipped with $\text{CuK}_{\alpha 1}$ radiation ($\lambda = 1.54056 \text{ \AA}$), curved germanium (111) Johann-type monochromator, and DECTRIS MYTHEN2 1K silicon strip detector. The phase purity of the $\text{Ce}_2\text{Ir}_3\text{Ga}_5$ samples was confirmed by an energy-dispersive x-ray spectroscopy (EDXS). Magnetization measurements were carried out using Quantum design SQUID in the temperature range 1.8–300 K and up to 7 T external field. AC transport and specific heat

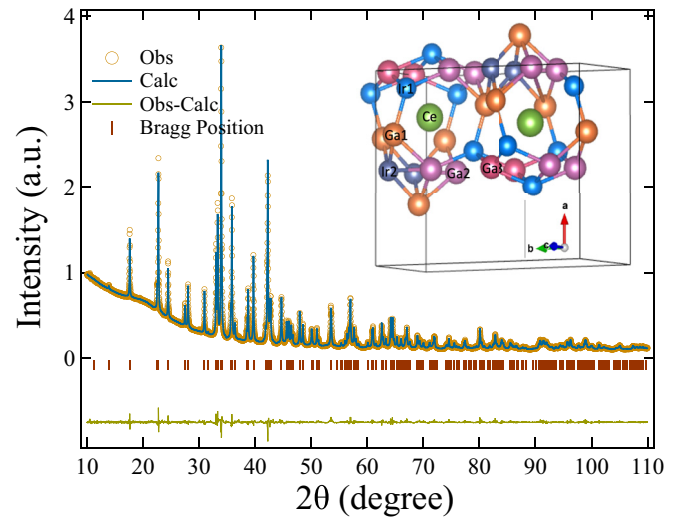


FIG. 1. Experimental powder XRD pattern of $\text{Ce}_2\text{Ir}_3\text{Ga}_5$ (yellow open circles) and the Rietveld refinement (blue solid line). Small red bars show the Bragg reflection positions, and a green solid line (bottom) shows the difference between the calculated and observed intensities. (b) Inset: Partial crystal structure showing the atomic arrangement around the Ce site (green sphere).

measurements were performed in a physical property measurement system (PPMS) equipped with a ^3He probe (0.5 K). Four-probe and two-tau relaxation methods were employed for AC transport and specific heat experiments, respectively.

III. RESULTS AND DISCUSSION

A. Structural characterization

Single-crystal XRD experiment was performed for crystal structure solution and refinement. A crystal of regular shape was fixed with glue at the top of a glass needle for x-ray diffraction intensity data collection. According to reflection conditions and isotypism to $\text{U}_2\text{Co}_3\text{Si}_5$ type [30,31], the crystal structure of $\text{Ce}_2\text{Ir}_3\text{Ga}_5$ was solved by direct methods using SHELXS [32] and refined using SHELXL [32] in the orthorhombic space group $Ibam$ (No. 72). Further results obtained from the analysis of crystallographic data are provided in Tables S1, S2, and S3 of Supplemental Material [33]. Powder x-ray diffraction (PXRD) intensities were collected for lattice parameter determination and phase purity analysis of $\text{Ce}_2\text{Ir}_3\text{Ga}_5$ bulk samples. Peak calibration followed by angle correction were performed on the PXRD pattern using the program WinXpow [34] and taking LaB_6 ($a = 4.1569 \text{ \AA}$) as an external standard. The lattice parameters $a = 10.0594(2) \text{ \AA}$, $b = 12.7239(3) \text{ \AA}$, $c = 5.7745(1) \text{ \AA}$ were determined by least-squares refinement on 169 reflection positions in the range of $5^\circ < 2\theta < 118^\circ$ using the software WinCSD [35]. Rietveld refinement on PXRD data (Fig. 1) was performed using the Fullprof software [36] by considering the crystallographic data obtained from the single crystal structure refinement. Some of the crystal structure parameters such as lattice constants and atomic positions obtained from the Rietveld refinement are shown in Table I. This result confirms quantitatively single-phase samples. The EDXS analysis, on polished pieces from both batches, results in good agreement

TABLE I. Structure parameters of Ce₂Ir₃Ga₅ obtained from powder XRD.

Structure	Orthorhombic				
Space group	<i>Ibam</i>				
Lattice parameters					
a (Å)	10.0594(2)				
b (Å)	12.7239(3)				
c (Å)	5.7745(1)				
V _{cell} (Å ³)	739.15(4)				
Atom	Wyckoff position	x/a	y/b	z/c	U _{iso/eq}
Ce1	8j	0.27267(5)	0.36125(4)	0	86(1)
Ir1	8j	0.09465(4)	0.14908(3)	0	88(1)
Ir2	4b	1/2	0	1/4	75(1)
Ga1	8j	0.3274(1)	0.0882(1)	0	89(2)
Ga2	8g	0	0.2943(1)	1/4	85(2)
Ga3	4a	0	0	1/4	92(3)

(Ce_{20.9}Ir_{29.7}Ga_{49.2}) with the stoichiometric composition of Ce₂₀Ir₃₀Ga₅₀ obtained from the crystal structure refinement. The crystal structure of the title compound (inset of Fig. 1) shows two important features: (i) a single cerium site and (ii) the absence of a local inversion center at the Ce site.

B. Magnetization

Magnetization measurements have been performed in the zero-field cooled mode. The temperature dependence of the inverse of susceptibility $\chi^{-1}(T)$ in 1 T external magnetic field is shown in Fig. 2. The high-temperature part (100 K $\leq T \leq$ 300 K) of $\chi^{-1}(T)$ shows a linear T dependence as expected for a local moment system. It can be well fitted with a modified Curie-Weiss equation: $\chi^{-1}(T) = (\chi_0 + \frac{C}{T-\theta_p})^{-1}$, where χ_0 is a temperature-independent contribution to the susceptibility, C is the Curie constant and θ_p is the

Curie-Weiss temperature. The fit yields a small $\chi_0 = 0.00038$ emu/mol, $C = 0.78(1)$ emu-mol_{Ce}/Oe, and $\theta_p = -184(1)$ K. The effective moment deduced from C is $\mu_{\text{eff}} = 2.5\mu_B$, which is close to the expected free ion value ($2.54\mu_B$) for Ce³⁺. Nonlinearity for $T < 100$ K is caused by crystal electric field (CEF) effects, i.e., a depopulation of excited CEF levels. There is no clear anomaly in the T dependence of the susceptibility, indicating the absence of a well-defined magnetic order. At small fields, there is a tiny kink in $\chi(T)$ at around 10 K. Because this anomaly is quite small, visible only at low fields, and there is no corresponding anomaly in other properties like resistivity or specific heat, we suspect this kink might originate from a tiny amount of disordered ferromagnetic (FM) foreign phase, which remained undetected in the EDXS measurements. While at low fields below 2 T, $\chi(T)$ continuously increases down to the lowest investigated temperatures, the application of higher fields results in the appearance of a maximum in $\chi(T)$ at around 4 K (upper inset of Fig. 2). Such a maximum in $\chi(T)$ has commonly been observed in Ce-based Kondo lattice systems located slightly on the nonmagnetic side of the QCP, like, e.g., CeRu₂Si₂ [37] or CeNi₂Ge₂ [38,39]. M(H) isotherms taken at different temperatures, 1.8 K, 50 K, and 120 K (lower inset of Fig. 2), all exhibit a linear increase with increasing field without signs of saturation up to the highest magnetic fields. In summary, the susceptibility results indicate a localized trivalent Ce state at higher temperatures without clear evidence for a magnetic ordering at low T .

C. Electrical resistivity

The temperature dependence of the electrical resistivity $\rho(T)$ of both Ce₂Ir₃Ga₅ and its non-f analog La₂Ir₃Ga₅ are shown in Fig. 3. The La-based compound displays the typical behavior of a standard metal, with a constant residual resistivity at low T and a linear increase due to phonon scattering at high T . Interestingly, it also shows a broadened transition to a superconducting state with an onset T_c and an offset T_c at about 0.75 K and 0.55 K, respectively. In contrast, $\rho(T)$ of Ce₂Ir₃Ga₅ is completely different, with an increase with decreasing T in the range 50 K $< T <$ 300 K, a broad maximum at around 30 K, followed by a strong

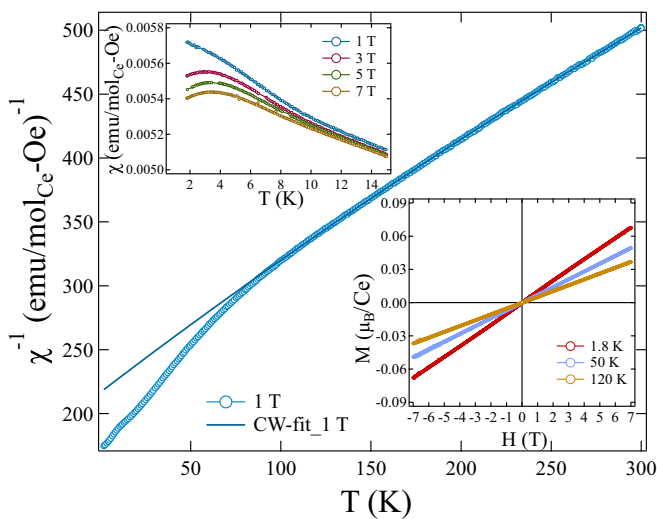


FIG. 2. Inverse susceptibility w.r.t. temperature in 1 T applied field is well described by a Curie-Weiss law in the high T regime. The inset on the top left represents $\chi(T)$ at different applied fields, whereas the inset on the bottom right displays MH curves measured at different temperatures 1.8 K, 50 K, and 120 K.

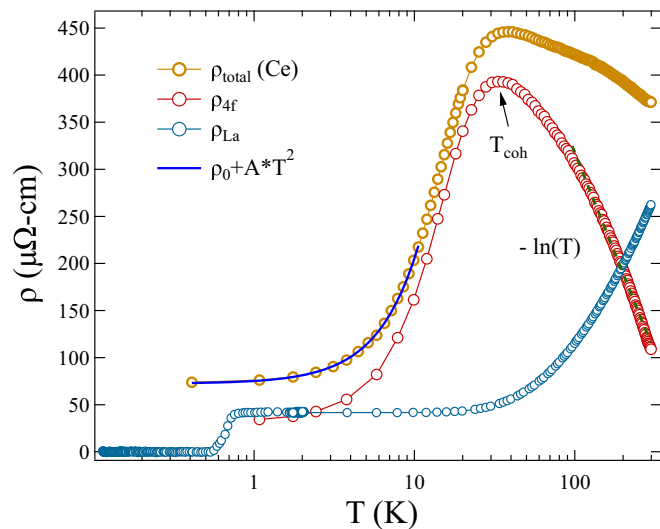


FIG. 3. Temperature dependence of electrical resistivity for $(\text{Ce, La})_2\text{Ir}_3\text{Ga}_5$ in zero applied fields where T is on a logarithmic scale. The total contribution to resistivity is shown by brown open circles, whereas the magnetic contribution is represented via red open circles.

decrease to lower T and a T^2 dependence below 10 K. This kind of temperature dependence is typical for a Kondo lattice system close to the QCP, but on the nonmagnetic side of the QCP. Since all these features are connected to the magnetic scattering of the $4f$ electrons, we tentatively estimated this magnetic contribution by subtracting $\rho(T)$ of $\text{La}_2\text{Ir}_3\text{Ga}_5$, making those features more apparent, especially at high T . There is an increase of ρ_{mag} with decreasing temperatures in the high-temperature region following a logarithmic behavior, as expected for an incoherent Kondo-type scattering. The maximum at around 30 K indicates the onset of coherence between the individual Kondo sites and is thus denominated by T_{coh} . Usually, it provides a first estimation of the Kondo energy scale, the Kondo temperature T_K . The slight bump in $\rho_{\text{mag}}(T)$ at about 150 K is likely connected with the Kondo scattering of excited CEF levels, suggesting the first excited CEF doublet to be in the range 150–300 K, a typical value for Cerium-based intermetallics. The strong decrease of ρ_{mag} below 20 K is due to the formation of a coherent Kondo state where the scattering of the Kondo sites gets in phase and thus becomes elastic. The T^2 dependence at low temperatures reflects the formation of a Fermi liquid. A fit with $\rho(T) = \rho_0 + A \times T^n$ gives $\rho_0 = 72.5 \mu\Omega \text{ cm}$, $A = 2.7 \mu\Omega \text{ cm K}^{-2}$, and $n = 1.7 \approx 2$ below 10 K. However, we are not confident about the absolute value of A and ρ_0 . The reason is that the absolute values of $\rho(T)$ at high T are larger than expected for such metallic systems [40,41]. We suspect this might be due to the formation of cracks within the sample, which reduces the effective width of the conduction channel and thus results in apparently high $\rho(T)$ values. However, such problems should not affect the resistivity ratios. Residual resistivity ratio (RRR) of 5 and 6 for $\text{Ce}_2\text{Ir}_3\text{Ga}_5$ and $\text{La}_2\text{Ir}_3\text{Ga}_5$, respectively, are typical for this kind of systems. They indicate some amount of impurities and/or defects, but with a level sufficiently low to allow for the formation of a well-defined coherent Fermi liquid ground state.

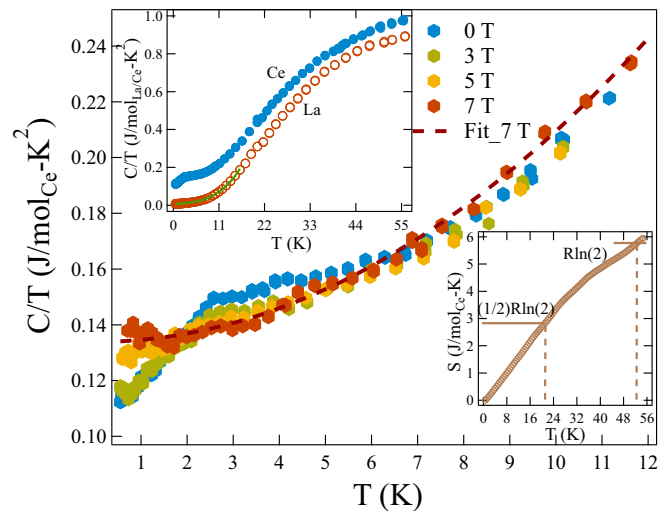


FIG. 4. C/T as a function of temperature in zero and different applied fields for $\text{Ce}_2\text{Ir}_3\text{Ga}_5$. The dashed line represents a fit to 7 T field data with $C/T = \gamma + \beta_3 T^2$. The lower inset shows the calculated entropy, whereas the upper inset displays the specific heat of $(\text{Ce, La})_2\text{Ir}_3\text{Ga}_5$ in zero field.

D. Specific heat

The upper inset in Fig. 4 displays temperature the dependence of specific heat C , normalized by temperature, $C(T)/T$, for $\text{Ce}_2\text{Ir}_3\text{Ga}_5$ and its non- $4f$ analog $\text{La}_2\text{Ir}_3\text{Ga}_5$ in zero applied fields. $\text{La}_2\text{Ir}_3\text{Ga}_5$ displays a standard metallic behavior where the high-temperature part is accounted by the phononic contribution and the lowest temperature region, which is nearly constant below 1.8 K, provides the electronic contribution. A fit to the data in the range $0.5 \text{ K} < T < 16 \text{ K}$ using $C/T = \gamma + \beta_3 T^2 + \beta_5 T^4$ where γ , β_3 , and β_5 are the electronic and phononic contributions, respectively is shown by green solid line. It provides $\gamma = 8.1 \text{ mJ}(\text{mol}_{\text{La}})^{-1} \text{ K}^{-2}$, a moderate value for metallic compounds, $\beta_3 = 0.34 \text{ mJ}(\text{mol}_{\text{La}})^{-1} \text{ K}^{-4}$, and $\beta_5 = 1.44 \mu\text{J}(\text{mol}_{\text{La}})^{-1} \text{ K}^{-6}$. By using the β_3 value, Debye temperature was calculated from the expression $\theta_D = (\frac{12\pi^4 RN}{5\beta_3})^{\frac{1}{3}} = 306 \text{ K}$, also a quite typical value for such a compound. There, $N = 5$, the number of atoms per formula unit according to per La mol, and R is the gas constant. The parameter β_5 accounts for the deviation of the phonon spectra from simple Debye spectra. The specific heat of $\text{La}_2\text{Ir}_3\text{Ga}_5$ did not exhibit a superconducting transition to the lowest-measured temperature (0.53 K), in contrast to $\rho(T)$ data. We suspect that the low T limit achieved in specific heat measurement, $T = 0.53 \text{ K}$, was not sufficiently low since the onset of the SC transition in $C(T)$ is usually only seen at the offset ($\rho = 0$) of the transition in $\rho(T)$.

In comparison, the specific heat of $\text{Ce}_2\text{Ir}_3\text{Ga}_5$ is larger than that of $\text{La}_2\text{Ir}_3\text{Ga}_5$ in the whole T range. The difference $C_{4f}(T) = C_{\text{Ce}}(T) - C_{\text{La}}(T)$ can be attributed to the effect of the $4f$ electrons. At first glance, it results in $C_{4f}(T)/T$ being only weakly T dependent in the investigated T range, reminiscent of a Fermi liquid behavior. This indicates that the $4f$ electrons do not behave as localized magnetic moments but instead hybridize strongly with the conduction electrons, forming heavy quasiparticles. Below 10 K, the C/T values

are in the order of $150 \text{ mJ}(\text{mol}_{\text{Ce}})^{-1}\text{K}^{-2}$, thus enhanced by a factor of 20 compared to the non- $4f$ analog La₂Ir₃Ga₅. It provides evidence that Ce₂Ir₃Ga₅ is a moderately heavy fermion system with strong f - c hybridization. By integrating $C_{4f}(T)/T$ we estimated the entropy $S_{4f}(T)$ connected with the $4f$ electrons (lower inset in Fig. 4). From the $J = 5/2$ multiplet for a localized Ce- $4f$ electron, one expects a high-temperature limit $S_{4f}(\infty) = R\ln 6$, but since the CEF splits this multiplet into three doublets, usually only the contribution $R\ln 2$ of the ground state doublet is recovered at lower T . In Ce₂Ir₃Ga₅, the $4f$ entropy increases continuously up to the highest investigated T , with only a small decrease in the slope above 35 K, and reaches $R\ln 2$ at about 52 K. This almost linear increase and the absence of saturation at $R\ln 2$ suggest that the energy scale of the f - c hybridization is similar to the CEF scale, resulting in a broadening and mixing of all CEF levels. The temperature $T(0.5R\ln 2) = 21 \text{ K}$ at which half of $R\ln 2$ is reached frequently provides a good estimate of the Kondo scale, with $T_K = 2T(0.5R\ln 2)$. This results in $T_K = 42 \text{ K}$, which is in reasonable agreement with the temperature of the maximum in $\rho(T)$. Thus, both the resistivity and the specific heat indicate Ce₂Ir₃Ga₅ to bear strong f - c hybridization resulting in a moderately heavy fermion system with a Kondo scale in the order of 40 K.

A closer look at the specific heat data at low T reveals a small kink in $C(T)/T$ at $T_0 \approx 2.7 \text{ K}$, below which $C(T)/T$ decreases with T , suggesting the presence of a phase transition at T_0 . The obvious question is whether this small anomaly is an intrinsic property of Ce₂Ir₃Ga₅, or due to a tiny amount of undetected foreign phase. The small size of this anomaly and the very small amount of entropy connected with this transition, only about 4% $R\ln 2$, favors the latter scenario. However, an analysis of the field dependence of C/T provides arguments in favor of the intrinsic nature of this transition. Application of a magnetic field $H > 3 T$ weakens this anomaly, seemingly without shifting T_0 to lower T , and at $7 T$, it can no longer be resolved (main part of Fig. 4). The suppression occurs in such a way that for $T < 0.5T_0$ the specific heat gets enhanced. At the same time, it gets suppressed above $0.5T_0$. At $7 T$ the experimental $C(T)$ can be nicely fitted with the standard function $C/T = \gamma + \beta_3 T^2$. The fit is represented by the red dashed line in the main part of Fig. 4. The obtained $\gamma_{7T} = 134 \text{ mJ}(\text{mol}_{\text{Ce}})^{-1}\text{K}^{-2}$ indicates a strong enhancement of the quasiparticles as previously stated. $\beta_3 = 0.75 \text{ mJ}(\text{mol}_{\text{Ce}})^{-1}\text{K}^{-4}$ is a factor of two larger than in La₂Ir₃Ga₅, which is likely due to additional strongly correlated contributions, connected, e.g., with CEF excitations. A check of the entropy $S(T, B)$ confirms that the entropy at 10 K is conserved, i.e., $S(10 \text{ K})$ is independent of the magnetic field. That means that the field-induced suppression of this transition is connected with a transfer of entropy gain from high $T > 0.5T_0$ in the ordered regime to low $T < 0.5T_0$ in the high field regime. For the magnetic order of a local moment magnetic system, one expects and usually observes precisely the opposite. In contrast, such a transfer of entropy to lower T is reminiscent of phase transitions in systems of itinerant electrons, e.g., a charge density wave (CDW) or an SC transition. The difference in C/T at the lowest T between the $7 T$ and the zero field curves amounts to about 20% of the C/T value at $7 T$. Assuming the transition to be intrinsic to Ce₂Ir₃Ga₅, that

would imply 20% of the density of states (DOS) of the heavy quasiparticles gets condensed, an amount quite typical, e.g., for a CDW transition. Assuming the transition to be due to a foreign phase, it would necessitate two conditions: firstly, that a substantial portion of the observed C/T at low T , exceeding 30%, is due to this foreign phase, and secondly, that a huge percentage of the DOS of this foreign phase gets condensed at T_0 . Both seem unlikely. Assuming the transition to be intrinsic to Ce₂Ir₃Ga₅, the very small size of the related anomaly and the condensed entropy would be in perfect accordance with the ordering temperature T_0 being one order of magnitude smaller than the Kondo temperature. We note that the closely related compound Ce₂Ru₃Ge₅ [42], which crystallizes in the same structure type, presents an FM heavy fermion ground state with $T_C = 7.9 \text{ K}$ and an estimated $T_K \approx 19 \text{ K}$. As mentioned in [43], there is a general relation between the $4f$ entropy collected at the magnetic ordering temperature T_M and the ratio T_M/T_K . The ratio $T_0/T_K \approx 0.1$ in Ce₂Ir₃Ga₅ is much lower than the ratio $T_C/T_K = 0.42$ in Ce₂Ru₃Ge₅. Accordingly, one expects the entropy at T_0 in Ce₂Ir₃Ga₅ to be much smaller than the entropy at T_C in Ce₂Ru₃Ge₅, and that is precisely what we observe. Thus Ce₂Ir₃Ga₅ could be a homolog of Ce₂Ru₃Ge₅ pushed very close to the critical point where the magnetic order disappears. From the total count of valence electrons, Ce₂Ir₃Ga₅ is close to Ce₂Ru₃Ge₅, since Ir has just one electron less than Ru. However, there is no clear evidence for the possible magnetic order in Ce₂Ir₃Ga₅ to be an FM one. Instead in Ce₂Ir₃Ga₅ both T_0 and the entropy recovery are shifted to lower T upon increasing the magnetic field. Both features are supportive for an anti-ferromagnetic (AFM) nature of the magnetic order, and contra-indicative for an FM state. Thus, Ce₂Ir₃Ga₅ would be a homologue of Ce₂Ru₃Ge₅ pushed to the critical magnetic point, but with an AFM order instead of an FM order. We note that there are closely related, isostructural Kondo systems that show AFM order instead of FM order, e.g., Ce₂(Rh/Ir)₃Ge₅ [44]. However, as the evidence in Ce₂Ir₃Ga₅ remains inconclusive, it is currently not feasible to definitively determine the nature of this transition, whether it is intrinsic or not.

IV. SUMMARY

We explored the Ce-Ir-Ga ternary system, in the search for a new cerium-based system that presents a locally non-centrosymmetric environment with preserved global inversion symmetry and has an appropriate strength of f - c hybridization so that an unconventional superconducting state like CeRh₂As₂ can be realized. There, the combination of Ir and Ga can provide the fine-tuned hybridization strength. This search leads to the discovery of a new compound Ce₂Ir₃Ga₅. Structural characterization revealed an orthorhombic U₂Co₃Si₅ structure type with space group: *Ibam*, No. 72. Magnetization measurements suggest a localized Ce³⁺ valence state at high temperatures but with no clear sign of magnetic ordering down to the lowest temperature. In AC transport measurements, $\rho(T)$ displays a typical Kondo behavior with a logarithmic increase in resistivity at high temperatures and a pronounced decrease below $T_{\text{coh}} \approx 30 \text{ K}$. Below 10 K, $\rho(T)$ follows a T^2 dependence, consistent with a Fermi liquid picture. Specific heat measurements evidence an enhanced

electronic contribution with an almost constant C/T value, $\gamma = 150 \text{ mJ}(\text{molCe})^{-1}\text{K}^{-2}$ in the range $3 \text{ K} < 30 \text{ K}$. This indicates strongly renormalized quasiparticles induced by a sizable f - c hybridization. From the T dependence of the entropy, we estimated a Kondo scale in the order of 42 K, which is in agreement with the temperature of the maximum in $\rho(T)$. Thus, resistivity and specific heat measurements indicate $\text{Ce}_2\text{Ir}_3\text{Ga}_5$ as a moderately heavy fermion system with a reasonably large Kondo scale. Susceptibility and resistivity measurements do not present any anomaly related to a transition, suggesting a paramagnetic heavy Fermi liquid ground state. However, specific heat data reveal a small anomaly at $T_0 = 2.7 \text{ K}$. At first glance, one would suspect this anomaly is due to a foreign phase. However, a more detailed analysis suggests

that it could also be due to an intrinsic itinerant type of order. Therefore, at present, we cannot conclude whether $\text{Ce}_2\text{Ir}_3\text{Ga}_5$ is on the magnetically ordered or the nonordered side of the quantum critical point. Further studies such as μSR and NMR experiments are needed. In addition, it will be interesting to observe whether further improvements in the sample quality result in the onset of unconventional superconductivity.

ACKNOWLEDGMENTS

We thank S. Kostmann and P. Scheppan for EDXS measurements, as well as S. Scharsach and M. Schmidt for performing DTA experiments.

-
- [1] E. Bauer and M. Sigrist, *Non-Centrosymmetric Superconductor: Introduction and Overview* (Springer-Verlag, Heidelberg, 2012).
- [2] M. Smidman, M. B. Salamon, H. Q. Yuan, and D. F. Agterberg, *Rep. Prog. Phys.* **80**, 036501 (2017).
- [3] F. Kneidinger, E. Bauer, I. Zeiringer, P. Rogl, C. B. Schenner, D. Reith, and, R. Podloucky, *Physica C* **514**, 388 (2015).
- [4] S. Fujimoto, *J. Phys. Soc. Jpn.* **76**, 051008 (2007).
- [5] E. Bauer, G. Hilscher, H. Michor, C. Paul, E. W. Scheidt, A. Griбанov, Y. Seropegin, H. Noël, M. Sigrist, and P. Rogl, *Phys. Rev. Lett.* **92**, 027003 (2004).
- [6] R. Settai, Y. Miyauchi, T. Takeuchi, F. Levy, I. Sheikin, and Y. Onuki, *J. Phys. Soc. Jpn.* **77**, 073705 (2008).
- [7] N. Kimura, K. Ito, H. Aoki, S. Uji, and T. Terashima, *Phys. Rev. Lett.* **98**, 197001 (2007).
- [8] M.-A. Méasson, H. Muranaka, T. D. Matsuda, T. Kawai, Y. Haga, G. Knebel, D. Aoki, G. Lapertot, F. Honda, R. Settai, J.-P. Brison, J. Flouquet, K. Shimizu, and Y. Onuki, *Physica C* **470**, S536 (2010).
- [9] F. Honda, I. Bonalde, K. Shimizu, S. Yoshiuchi, Y. Hirose, T. Nakamura, R. Settai, and Y. Onuki, *Phys. Rev. B* **81**, 140507(R) (2010).
- [10] N. Kanazawa, S. Seki, and Y. Tokura, *Adv. Mater.* **29**, 1603227 (2017).
- [11] H. Ninomiya, Y. Matsumoto, S. Nakamura, Y. Kono, S. Kittaka, T. Sakakibara, K. Inoue, and S. Ohara, *J. Phys. Soc. Jpn.* **86**, 124704 (2017).
- [12] J. Železný, H. Gao, K. Výborný, J. Zemen, J. Mašek, A. Manchon, J. Wunderlich, J. Sinova, and T. Jungwirth, *Phys. Rev. Lett.* **113**, 157201 (2014).
- [13] H. Watanabe and Y. Yanase, *Phys. Rev. B* **96**, 064432 (2017).
- [14] A. Generalov, J. Falke, I. A. Nechaev, M. M. Otrokov, M. Güttler, A. Chikina, K. Kliemt, S. Seiro, K. Kummer, S. Danzenbächer, D. Usachov, T. K. Kim, P. Dudin, E. V. Chulkov, C. Laubschat, C. Geibel, C. Krellner, and D. V. Vyalikh, *Phys. Rev. B* **98**, 115157 (2018).
- [15] M. H. Fischer, F. Loder, and M. Sigrist, *Phys. Rev. B* **84**, 184533 (2011).
- [16] D. Maruyama, M. Sigrist, and Y. Yanase, *J. Phys. Soc. Jpn.* **81**, 034702 (2012).
- [17] Y. Mizukami, H. Shishido, T. Shibauchi, M. Shimozawa, S. Yasumoto, D. Watanabe, M. Yamashita, H. Ikeda, T. Terashima, H. Kontani, and Y. Matsuda, *Nat. Phys.* **7**, 849 (2011).
- [18] M. H. Fischer, M. Sigrist, D. F. Agterberg, and Y. Yanase, *Annu. Rev. Condens. Matter Phys.* **14**, 153 (2023).
- [19] K. Nogaki and Y. Yanase, *Phys. Rev. B* **106**, L100504 (2022).
- [20] D. Möckli and A. Ramires, *Phys. Rev. B* **104**, 134517 (2021).
- [21] T. Yoshida, M. Sigrist, and Y. Yanase, *Phys. Rev. B* **86**, 134514 (2012).
- [22] S. Khim, J. F. Landaeta, J. Banda, N. Bannor, M. Brando, P. M. R. Brydon, D. Hafner, R. Kuchler, R. Cardoso-Gil, U. Stockert, A. P. Mackenzie, D. F. Agterberg, C. Geibel, and E. Hassinger, *Science* **373**, 1012 (2021).
- [23] S.-I. Kimura, J. Sichelschmidt, and S. Khim, *Phys. Rev. B* **104**, 245116 (2021).
- [24] S. Kitagawa, M. Kibune, K. Kinjo, M. Manago, T. Taniguchi, K. Ishida, M. Brando, E. Hassinger, C. Geibel, and S. Khim, *J. Phys. Soc. Jpn.* **91**, 043702 (2022).
- [25] S. Onishi, U. Stockert, S. Khim, J. Banda, M. Brando, and E. Hassinger, *Front. Electron. Mater.* **2**, 880579 (2022).
- [26] D. Hafner, P. Khanenko, E.-O. Eljaouhari, R. Kuchler, J. Banda, N. Bannor, T. Lühmann, J. F. Landaeta, S. Mishra, I. Sheikin, E. Hassinger, S. Khim, C. Geibel, G. Zwicknagl, and M. Brando, *Phys. Rev. X* **12**, 011023 (2022).
- [27] K. Semeniuk, D. Hafner, P. Khanenko, T. Lühmann, J. Banda, J. F. Landaeta, C. Geibel, S. Khim, and E. Hassinger, and M. Brando, *Phys. Rev. B* **107**, L220504 (2023).
- [28] D. Aoki, J.-P. Brison, J. Flouquet, K. Ishida, G. Knebel, Y. Tokunaga, and Y. Yanase, *J. Phys.: Condens. Matter* **34**, 243002 (2022).
- [29] H. G. Suh, Y. Yu, T. Shishidou, M. Weinert, P. M. R. Brydon, and D. F. Agterberg, *Phys. Rev. Res.* **5**, 033204 (2023).
- [30] L. G. Aksel'rud, Y. P. Yarmolyuk, and E. I. Gladyshevskii, *Sov. Phys. Crystallogr.* **22**, 492 (1977).
- [31] L. Piraux, E. Grivei, B. Chevalier, P. Dordor, E. Marquestaut, and J. R. Etourneau, *J. Magn. Magn. Mater.* **128**, 313 (1993).
- [32] G. M. Sheldrick, SHELXS97 and SHELXL97, University of Göttingen, Germany, Acta Crystallographica Section E Structure Reports, 1997.
- [33] See Supplemental Material at <http://link.aps.org/supplemental/10.1103/PhysRevMaterials.8.085001> for detailed information about crystal structure determination, synthesis and specific heat measurements on various batches.

- [34] STOE and Cie, STOE Powder Diffraction Software Package WinXPOW, ver.2.25 (2009).
- [35] L. Akselrud, Y. Grin, WinCSD: software package for crystallographic calculations (Version 4), *J. Appl. Crystallogr.* **47**, 803 (2014).
- [36] J. Rodriguez-Carvajal, FULLPROF program, FULLPROF program, *Satellite Meeting on Powder Diffraction of the XVth Congress of the IUCr, Toulouse, France*, 1990.
- [37] P. Haen, J. Flouquet, F. Lapierre, and P. Lejay, *J. Low Temp. Phys.* **67**, 391 (1987).
- [38] T. Fukuhara, K. Maezawa, H. Ohkuni, J. Sakurai, H. Sato, H. Azuma, K. Sugiyama, Y. Ōnuki, and K. Kindo, *J. Phys. Soc. Jpn.* **65**, 1559 (1996).
- [39] T. Fukuhara, K. Maezawa, H. Ohkuni, J. Sakurai, and H. Sato, *J. Magn. Magn. Mater.* **140-144**, 889 (1995).
- [40] R. Kurlito, A. Szytuła, J. Goraus, S. Baran, Y. Tyvanchuk, Y. M. Kalychak, P. Starowicz, *J. Alloys Compd.* **803**, 576 (2019).
- [41] A. Kowalczyk, V. H. Tran, T. Toliński, and W. Miiller, *Solid State Commun.* **144**, 185 (2007).
- [42] R. K. Kamadurai, R. D. Fobasso, A. Maurya, P. K. Ramankutty, and A. M. Strydom, *J. Phys. Soc. Jpn.* **89**, 064705 (2020).
- [43] H. Yashima, H. Mori, N. Sato, T. Satoh, and K. Kohn, *J. Magn. Magn. Mater.* **31-34**, 411 (1983).
- [44] Z. Hossain, H. Ohmoto, K. Umeo, F. Iga, T. Suzuki, T. Takabatake, N. Takamoto, and K. Kindo, *Phys. Rev. B* **60**, 10383 (1999).